Positron annihilation studies of 4-*n*-butyl-4′-isothiocyanato-1,1′-biphenyl

E. Dryzek,[1] E. Juszyńska,[1] R. Zaleski,[2] B. Jasińska,[2] M. Gorgol,[2] and M. Massalska-Arodź[1]
[1]*The H. Niewodniczański Institute of Nuclear Physics PAN, ul. Radzikowskiego 152, 31-342 Kraków, Poland*
[2]*Institute of Physics, Marii Curie-Skłodowska University, Pl. M. Curie-Skłodowskiej 1, 20-031 Lublin, Poland*
(Received 17 May 2013; published 19 August 2013)

Positron annihilation lifetime spectroscopy (PALS) measurements were performed between 93 and 293 K in order to study the supercooled smectic-*E* (Sm-*E*) phase of 4-*n*-butyl-4′-isothiocyanato-1,1′-biphenyl (4TCB), the ordered molecular crystal of 4TCB, and the phase transition between the Sm-*E* phase and the ordered molecular crystal of 4TCB. The phase transition was well reflected in the abrupt increase of the *ortho*-positronium (*o*-Ps) lifetime and intensity. The value of the *o*-Ps lifetime in the Sm-*E* liquid crystalline phase of 4TCB, i.e., 2.21 ns at room temperature, was explained by the formation of bubbles induced by Ps atoms, which are created due to a liquidlike state of the butyl chains of 4TCB molecules in the Sm-*E* phase. The temperature dependence of the *o*-Ps intensity for the supercooled Sm-*E* phase can be explained by thermal generation of sites where bubbles are formed; an activation energy equal to 0.30 ± 0.02 eV was estimated. This value was compared with the activation energies of molecular motions. The *o*-Ps lifetime in the ordered molecular crystal was interpreted as originating from the annihilation of *o*-Ps confined in molecular vacancy-type imperfections in the crystal lattice. The value of the *o*-Ps pickoff annihilation between 1.8 and 1.9 ns is in accordance with the size of the molecular vacancy for the 4TCB crystal lattice. Its intensity is lower than 5%. The isothermal crystallization of the 4TCB Sm-*E* phase was observed by PALS. The low-dimensional crystal growth was concluded from the Avrami equation fitted to the time dependence of the *o*-Ps intensity, which resulted in an Avrami exponent equal to 1.73.

DOI: 10.1103/PhysRevE.88.022504 PACS number(s): 83.80.Xz, 78.70.Bj, 64.70.dg

I. INTRODUCTION

Positron annihilation is a useful technique for studies of various molecular substances. It allows determining structural changes related to changes of local electronic structure of the material at an atomic level [1–3]. The bound state of the positron and electron, i.e., positronium (Ps), forms in two spin states. *Para*-positronium (*p*-Ps) with antiparallel spins of its two constituting particles has an intrinsic lifetime in vacuum equal to 125 ps and annihilates into two photons. The bound state with parallel particle spins, i.e., *ortho*-positronium (*o*-Ps), whose lifetime in vacuum is equal to 142 ns, annihilates into three photons. The relative abundance of these two states is 1:3. It is commonly accepted that in molecular substances Ps is formed in subnanometer-size free volumes, i.e., voids with low electron density, and its positron can annihilate with an electron of the surrounding molecules. This process, called pickoff annihilation, causes a reduction of *o*-Ps lifetime to several nanoseconds. A typical positron lifetime spectrum for a molecular substance contains three components. The pickoff annihilation of *o*-Ps constitutes still the longest component of order of a few nanoseconds. The other two components with values close to 125 ps and several hundreds of picoseconds (usually lower than 0.5 ns) come from *p*-Ps annihilation and free positron annihilation, respectively. It was established that the lifetime of *o*-Ps is very sensitive to the local free volume size and thus *o*-Ps is used as a probe of size and concentration of these free volumes. Positron annihilation was also successfully applied in the study of liquid crystals [4].

For liquid crystalline materials, it was observed that both *o*-Ps lifetime and its relative intensity are very sensitive not only to the phase transition between the ordered molecular crystal and liquid crystal or the liquid crystal and isotropic liquid, but also to phase transformations between different mesophases [4–6] including changes of internal molecular ordering even without any substantial free volume or macroscopic density changes. The fact that *o*-Ps is sensitive to microscopic properties and local arrangement of molecules in liquid crystals is probably related to the dipolar character of the molecules.

In this work we used positron annihilation lifetime spectroscopy (PALS) for studies of C_4H_9-C_6H_4-C_6H_4-NCS (4TCB), which is a compound from the homologous series 4-*n*-alkyl-4′-isothiocynato-1,1′-biphenyl (C_nH_{2n+1}-C_6H_4-C_6H_4-NCS, abbreviated as *n*TCB) showing one soft crystalline phase, called the smectic-*E* (Sm-*E*) phase, around room temperature for $n = 2$–10 [7,8]. For 4TCB, the Sm-*E* phase can be cooled down to liquid-nitrogen temperature, which is below the expected transition temperature between the ordered crystalline phase and the Sm-*E* phase. The Sm-*E* phase is found in compounds consisting of rodlike molecules similarly to liquid crystalline phases, i.e., nematic, smectic-*A*, and smectic-*C* phases. For 4TCB the crystal-like Sm-*E* phase, called also Cry-*E*, is characterized by the orthorhombic arrangement of molecules orthogonal within the smectic layers. There is long-range positional ordering within layers and between them concerning molecular centers. Initially, in contrast to other compounds of the *n*TCB homologous series, no ordered crystalline phase had been reported under ambient pressure; the ordered crystalline phase was formed only under high pressure above 88.7 MPa [9]. Eventually, the ordered crystalline phase was obtained after long time annealing of the sample below 250 K [10]. It was confirmed also by x-ray-powder-diffraction experiments [11].

The molecular dynamics in the Sm-*E* phase has been investigated using dielectric relaxation [7,12,13], NMR [10], and quasielastic neutron scattering measurements [11]. A very slow motion identified as the molecular reorientation around the molecular short axis, flipping motion of phenyl rings,

translational diffusion and libration around the molecular long axis were observed [10]. Previous x-ray-diffraction studies have shown that even the molecular rotation around its long axis should be restricted [8,13].

The possibility of the Sm-E phase glass occurrence for 4TCB was reported previously [10]. A hypothesis was formed that in the Sm-E phase of glass the smectic layer system is sustained, but the orthorhombic order of the molecules in the layers is slightly disturbed. The vitreous state of the Sm-E phase is most probably formed upon freezing of the molecular reorientations and fluctuations of structural disorder. Since PALS is widely used for studies of local free volume changes accompanying the glass transition in polymers [14,15] and low molecular glass formers [14,16] and it is sensitive to the local arrangement of molecules in liquid crystals, those measurements could shed light on the possible formation of a glass state of the Sm-E phase.

The main aim of our research is to characterize the microstructure of the local free volumes in 4TCB and their changes with temperature for the supercooled Sm-E phase, searching for glass transition as well as observation of crystallization of the Sm-E phase and melting of the ordered molecular crystal using PALS.

II. EXPERIMENTAL DETAILS

A. Materials

The 4TCB substance was synthesized according to Ref. [7] at the Institute of Chemistry, the Military University of Technology in Warsaw and used as obtained for PALS measurements. The sample was a liquid crystal at room temperature.

B. Positron lifetime measurements

Positron annihilation lifetime spectra were measured using a standard fast-slow delayed coincidence setup with BaF_2 scintillation detectors. The resolution function was single Gaussian with a full width at half maximum equal to 255 ps, checked by ^{60}Co isotope measurement. The positron source of activity of 50 μCi enclosed in an 8-μm Kapton foil was sandwiched between the samples of 4TCB and placed in the measurement chamber. In the chamber the air pressure was kept at a level of 0.5 Pa. The measurements were performed in the temperature range between 93 and 293 K. The temperature was measured by a thermo-couple inserted in the copper wall of the sample container.

The obtained PALS spectra containing 10^6 counts were analyzed with the help of the LT program [17] assuming that the spectrum consisted of three exponential components convoluted with the instrumental resolution curve and constant random coincidence background. The shortest-lived component was ascribed to p-Ps decay, the intermediate one to the annihilation of free positrons, and the longest-lived one to o-Ps decay mostly due to the pickoff process. In order to reduce the number of free parameters the p-Ps to o-Ps intensity ratio was set to 1:3 according to the statistical weights of these states. The lifetime of the source component was equal to 374 ps and its intensity was set to 10.2%, based on the calculations according to Ref. [18], which were taken into account in the deconvolution of the spectra. The weak dependence of the positron lifetime in Kapton on temperature, which can influence only the free positrons annihilation component, was neglected [19].

1. *Measurement for the supercooled Sm-E phase*

The first measurement was performed for the supercooled Sm-E phase. To obtain the supercooled sample its temperature was reduced at a rate of 5 K/min from room temperature to 93 K. The 1-h measurements of the positron lifetime spectra were performed on heating of the sample at temperature intervals of 10 K starting from 93 K. Before a measurement the sample was kept at a given temperature for approximately 10 min. In the vicinity of the phase transition temperature, i.e., 284.1 K [10], the temperature interval was reduced to 5 K.

2. *Crystallization procedure and measurements*

The preparation for crystallization of the Sm-E sample consisted of cooling of the sample to 93 K at a rate of 1 K/min and then heating it from 93 to 253 K with the same rate. The sample was kept at this temperature for 48 h. The procedure was performed for the sample and the positron source located in the measuring chamber. This gave us the opportunity to record the positron lifetime spectra, which were registered in 2-min intervals during cooling and heating of the sample. The short measuring time caused a low number of counts in these spectra. This did not allow us to analyze them conventionally and obtain the values of positron lifetime components and their intensities. However, the total number of counts in the region of the spectrum where the main contribution comes from the o-Ps annihilation provides useful information about the behavior of this positron lifetime component. It is approximately proportional to the intensity of this component. For the component with the intensity I and lifetime τ the number of counts in the time range between t_1 and t_2 is given by $A = I[\exp(-t_1/\tau) - \exp(-t_2/\tau)] \cong I \exp(-t_1/\tau)$ when t_2 is a few times higher than t_1. In our case the main contribution to the change in A, which increases about 40 times, comes from the change in intensity I. The change of the lifetime from 1.4 to 2.2 ns (as it is in our case) without the change in intensity I would cause an increase of A less than 2 times. Figure 1 shows examples of the spectra and the chosen time range, i.e., between 2.2 and 8.2 ns. After 48 h the sample temperature was lowered to 248 K and crystallization started, indicated by the decreasing number of counts in the above-mentioned time range. During crystallization the positron lifetime spectra were registered. After crystallization the temperature of the sample was lowered to 93 K and a measurement cycle similar to that for the supercooled Sm-E phase was performed for the ordered molecular crystal sample.

III. RESULTS AND DISSCUSION

Due to Coulomb and exchange forces, Ps formed in molecular solids and liquids is repelled from the molecules into the free volume surrounding them. In perfect crystals with an open structure they may be interstitial regions, e.g., empty space between lattice plains. Thus the lifetimes should be those of o-Ps in the bulk of the crystals. Open volume

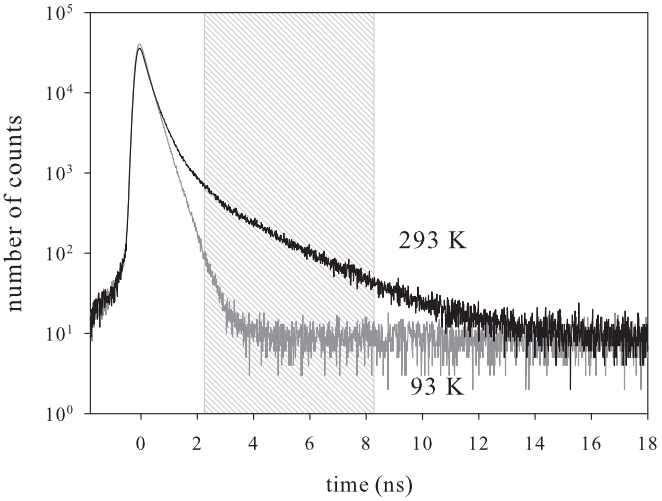

FIG. 1. Positron lifetime spectra for the Sm-*E* phase of 4TCB at temperatures of 93 K (gray line) and 293 K (black line). The hatched area shows the time range between 2.2 and 8.2 ns, where the main contribution to the spectrum comes from the *o*-Ps annihilation.

lattice imperfections such as thermally generated molecular vacancies or divacancies can localize *o*-Ps and its lifetime depends on the vacancy size [2]. Due to structural disorder in amorphous molecular solids such as amorphous polymers or molecular glasses Ps is trapped by the holes of the excess free volume, which are inter- and intramolecular regions characterized by lower electron density [15].

Thus the main discussion of results will deal with the behavior of the *o*-Ps lifetime τ_3 and its intensity I_3. Assuming that pickoff is the main process of *o*-Ps annihilation and other quenching mechanisms of *o*-Ps such as *ortho-para* spin conversion in internal or external magnetic fields or chemical quenching are negligible, i.e., $\tau_3 = \tau_{po}$, the free volume hole radius R may be calculated according to the semiempirical model [20,21], which relates the pickoff lifetime τ_{po} (in ns) to the free volume radius of a spherical hole $v_h = 4\pi R_0^3/3$:

$$\tau_{po} = \tfrac{1}{2}\{1 - R_0/(R_0 + \Delta R) + (1/2\pi)\sin[2\pi R_0/(R_0 + \Delta R)]\}^{-1}, \quad (1)$$

where the parameter $\Delta R = 0.166$ nm is an empirical parameter.

Figure 2 presents the τ_3 and I_3 dependences on temperature for the Sm-*E* phase and ordered crystalline phase of 4TCB. These results will be discussed in the next two subsections. In Fig. 2(a) the right vertical axis displays the values of the free volume hole radius R corresponding to the τ_3 values according to Eq. (1).

A. Annealing of the supercooled Sm-*E* phase

The PALS measurements for the Sm-*E* phase started at the temperature of 93 K, but for temperatures lower than 163 K the positron lifetime spectrum exhibits only a single lifetime component related to positron annihilation in a free state. Its value slightly increases from 0.384 ± 0.001 to 0.393 ± 0.001 ns with an increase in temperature from 93 to 153 K. For higher temperatures the positron lifetime

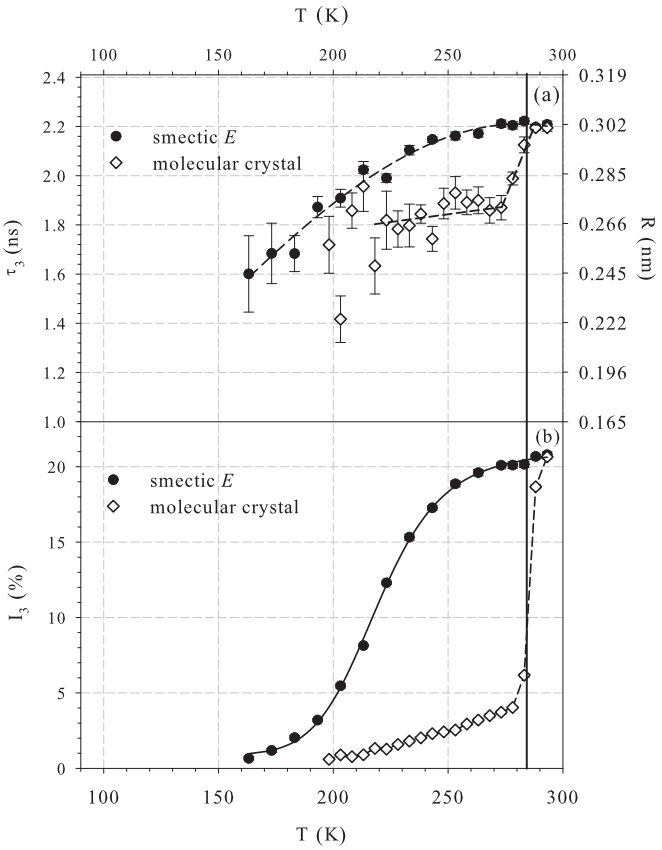

FIG. 2. Temperature dependences of (a) τ_3 and (b) I_3 for the Sm-*E* and ordered crystalline phases of 4TCB. The right vertical axis shows the values of the free volume radius R calculated from Eq. (1). The solid line is the fit of the relation given by Eq. (4) to the experimental points. The dashed lines are meant as guides for the eye. The black vertical line indicates the temperature of the ordered crystal – Sm-*E* phase transition determined by the heat capacity measurements [10], i.e., 284.1 K.

spectrum exhibits three components. The second component τ_2 coming from positron annihilation in a free state continues to increase smoothly to 0.403 ± 0.003 ns at 203 K and then to 0.468 ± 0.003 at 293 K. The third component τ_3 has an intensity lower than 1% and a value of 1.6 ns at a temperature of 163 K. Then τ_3 increases with temperature and saturates in the vicinity of the phase transition temperature, reaching the value of 2.21 ns at 293 K, as depicted in Fig. 2 (closed circles).

The lifetime of 2.21 ns resulting from the pickoff annihilation of *o*-Ps indicates the radius of the spherical free volume $R = 0.30$ nm and $v_h = 0.117$ nm^3 according to Eq. (1). In order to establish the *o*-Ps location in the structure of the 4TCB Sm-*E* phase the size of this spherical free volume was compared with average spacing between the smectic layers. Taking into account the molecule length $L = 1.659$ nm [8] and the lattice constant $c = 1.816$ nm for the Sm-*E* phase at a temperature of 333 K, the estimated separation of the adjacent smectic layers is equal to $c - L = 0.157$ nm, which is almost a quarter the diameter of the free volume detected by *o*-Ps.

Lightbody *et al.* [22] established the following empirical relation for some molecular crystals, e.g., low molar mass

hydrocarbon crystals:

$$\tau_{po} = 7.92 - 9.61k. \quad (2)$$

where the packing coefficient k, defined as the fraction of volume occupied by molecules, is related to the o-Ps lifetime (in ns). The packing coefficient for the Sm-E phase is equal to 0.623 at 333 K [8]. Then the o-Ps lifetime obtained from Eq. (2) is equal to 1.93 ns. Taking into account the thermal expansion coefficient for the Sm-E phase $\alpha = 5 \times 10^{-4}\,\mathrm{K}^{-1}$, the o-Ps lifetime would be 1.81 ns at 293 K. These values are lower than the 2.21 ns obtained from the measurement at 293 K. An explanation of the o-Ps lifetime that is longer than expected requires taking into account liquid properties of the Sm-E phase.

In liquids Ps is confined in a free volume, i.e., "a bubble," that Ps forms itself due to repulsion by molecules. The so-called bubble model of Ps formation was proposed by Ferrell [23] to explain the unexpectedly long lifetime of the o-Ps in liquid helium. According to this model, strong exchange repulsion between the o-Ps electron and electrons of the surrounding He atoms was approximated by a spherically symmetric potential well of radius R. The equilibrium radius R_{eq} of the bubble is determined by the minimum of the sum of the Ps energy, the surface energy, and the energy related to the external pressure, which is negligible in this case. The following relationship is obtained for the equilibrium radius of the bubble:

$$R_{eq} = \left(\frac{\pi\hbar^2}{16 m_0 \sigma}\right)^{1/4}, \quad (3)$$

where σ is the surface tension and m_0 is the electron mass. For nonpolar liquids of symmetrical molecules $R_{eq} \approx R_0 + \Delta R$.

The values of macroscopic surface tension measured for different smectic liquid crystals are in the range between 19×10^{-3} and 28×10^{-3} N/m [24]. For smectic liquid crystals the surface tension is a tensor and measured values are certain components of this tensor along the smectic layer normal. Following that, the radius of the bubble induced by Ps, R_{eq} from Eq. (3), would be in the range between 0.59 and 0.54 nm. These values are higher compared to the $R_0 + \Delta R$ obtained for the Sm-E phase of 4TCB from Eq. (1). This may be caused by the presence of the strongly polar groups NCS with the dipole moment 3.5 D. Moreover, the bubble of a radius of 0.3 nm or smaller is surrounded by a small number of molecules and its radius of curvature may significantly affect the surface tension. In that case the microscopic value of the surface tension should be considered. Thus the approach presented above does not give a comprehensive explanation of the o-Ps lifetime in the 4TCB Sm-E phase and in particular it does not identify sites of Ps confinement. However, the observed increase of τ_3 and then the bubble radius with temperature may be related to a decrease in surface tension.

The dependence of the intensity I_3 on temperature (closed circles) depicted in Fig. 2(b) exhibits a sigmoidal shape. This type of dependence suggests that o-Ps formation is a thermally activated process, i.e., the centers where o-Ps is formed and annihilates are thermally activated equilibrium defects. Similar dependences characterize, for example, thermal vacancy formation. We propose to describe the obtained dependence

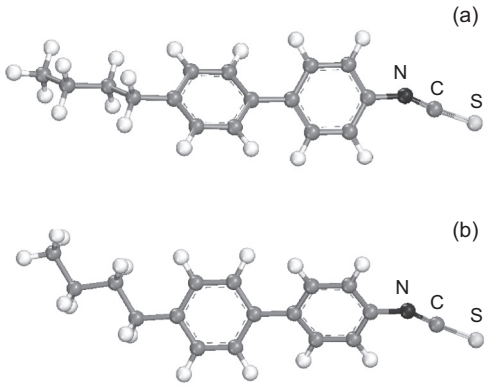

FIG. 3. Molecular structure of 4TCB optimized by b3lyp/6-311G** for (a) *trans* and (b) *gauche* conformations.

by the following equation:

$$I_3(T) = \frac{I_0 + I_{\mathrm{sat}} A \exp\left(-\frac{E_a}{k_B T}\right)}{1 + A \exp\left(-\frac{E_a}{k_B T}\right)}, \quad (4)$$

where I_0 is the initial value of I_3, I_{sat} is the saturated value of I_3, A is a constant coefficient, k_B is the Boltzmann constant, and E_a can be treated as the activation energy. The solid line in Fig. 2(b) was obtained by fitting Eq. (4) to the experimental data. The value of E_a obtained from the fit is equal to 0.30 ± 0.02 eV and the constant A is equal to $(4.9 \pm 2.7) \times 10^6$.

The questions arise as to where in the Sm-E structure of 4TCB the o-Ps presence causes bubble formation and which process is responsible for the temperature dependence of o-Ps intensity. Differential scanning calorimetry and Fourier transform infrared spectroscopy studies of nTCB compound homologous series [25,26] showed that alkyl chains of nTCB are already molten in the Sm-E phase by the same degree as in isotropic liquid. Additionally, the orientational order of molecules is partially lost in the Sm-E phase in comparison to the ordered crystalline phase. The head-to-tail orientations of molecules are disordered.

In order to find out about the possible sites of bubble formation in the Sm-E phase of 4TCB the geometry of an isolated molecule has been optimized using the DMol3 program by the density-functional Perdew-Burke-Ernzerhof (PBE) correlation [27] with the gradient-corrected (generalized gradient approximation) basis set [28,29]. The structures of the lowest-energy conformers of the 4TCB molecule calculated on the PBE level are displayed in Fig. 3. A crankshaft-type conformation change within the left-hand side of the alkyl chain was simulated by a molecular mechanics calculation for the smectic phase, with the right-hand side of the chain assumed rigid. Also possible are CH_3 group motions and alkyl chain changes correlated with a vibration-reorientation coupling, which could also contribute to the mobility of the chain. On the basis of calculations the energy barrier to this type of motion is low, i.e., 0.13 eV. It seems that conformational changes of the butane chain can create a convenient site for Ps, e.g., the space between the smectic layers, which contain molecules of *trans* and *gauche* conformations, is sufficient to inscribe the sphere of radius of 0.28 nm for the lattice constants close to those given in Ref. [8]. This is shown in Fig. 4. The π

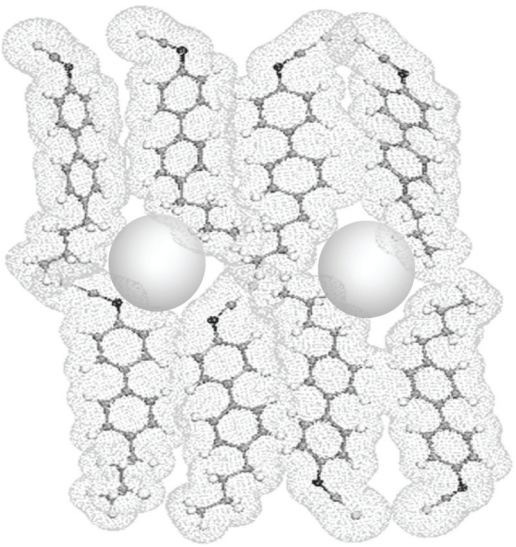

FIG. 4. Arrangement of eight molecules of 4TCB in the Sm-*E* phase forming a fragment of two horizontal smectic layers perpendicular to the figure plane. The lattice constants for the Sm-*E* phase are $a = 0.80$ nm, $b = 0.55$ nm, and $c = 1.82$ nm. The gray area depicts the van der Waals volumes of molecules. Spheres of radius of 0.28 nm indicate possible sites confining Ps.

electron density of the NCS groups can hinder Ps formation, but head to tail disorder can create a shell of a few butyl chains.

It seems that regions of alkyl chains are the sites where bubbles induced by Ps atoms are formed also in other liquid crystals as it was found for the triple-chain amphiphilic diol **1** liquid crystal [6]. In this compound Ps is formed in the regions of hydrophobic alkyl chains that are in the mobile liquidlike state and its lifetime, slightly higher than 3 ns, is close to values observed for liquid alkanes. The influence of the electric field on the free volume properties of the nematic phase of 4-cyano-4′-*n*-pentylbiphenyl (5CB) was investigated by Zhao and Ujhira [30]. In comparison to 4TCB, 5CB has five carbon atoms in the alkyl chain and another similarly strong polar group –CN at the terminal position. Application of a direct electric field to the sample caused an increase of the *o*-Ps lifetime from 2.2 to 2.6 ns and a decrease of its intensity from 12.5% to 6.5%. The authors suggested that orientation of molecules along the electric field direction resulted in the creation of larger bubbles induced by Ps atoms between the alkyl chains of molecules and the decrease of the *o*-Ps intensity is connected to the lower concentration of such places.

Since conformational changes and molecular motions can create sufficient space for Ps formation it is interesting to compare the activation energy E_a obtained by fitting Eq. (4) with activation energies of the molecular motions. The ^{1}H NMR T_1 studies of the Sm-*E* phase of 4TCB [10] indicated four motional modes of molecules: methyl reorientation with $E_a = 0.093 \pm 0.005$ eV, flipping of phenyl rings or tumbling of the alkyl group with $E_a = 0.19 \pm 0.02$ eV, reorientation around the long axis with $E_a = 0.21 \pm 0.02$ eV, and head-to-tail reorientation around the short axis with $E_a = 0.98 \pm 0.10$ eV. The reorientation of the longitudinal dipole moments of molecules around the short axis with the activation energy 0.84 ± 0.05 eV was also observed in dielectric relaxation studies [12]. The value of 0.30 ± 0.02 eV is higher than the activation energies of the second and third modes. However, the subsequent discussion of the fast PALS measurements on cooling and heating of the sample during preparation for crystallization indicates that the thermal equilibrium of the sample might be incomplete and the activation energy obtained from the I_3 temperature dependence may be slightly lower than 0.30 ± 0.02 eV and closer to the values of the activation energies for the second and third modes of molecular motion distinguished by Ishimaru *et al*. [10].

It is also worth noticing that the temperature range of the I_3 growth, i.e., between 163 and 263 K [see Fig. 2(b)], is similar to that in which the heat capacity of the quenched Sm-*E* phase exhibits a hump, i.e., between 150 and 250 K [10]. This anomaly was previously suggested to be due to a glass transition consisting in freezing in the head-to-tail disorder [12]. However, according to Ishimaru *et al*. [10], it lacks other typical thermodynamic signatures of the glass transition observed in adiabatic calorimetry so it was indicated as corresponding to a higher-order transition.

It is interesting that a similar dependence of the *o*-Ps annihilation intensity on temperature was observed for polycrystalline aromatic hydrocarbons such as biphenyl, *p*-terphenyl, and quaterphenyl [31]. In that case the long-lived lifetime component appeared in the spectra on heating only above some temperature with a much lower value, i.e., slightly higher than 0.6 ns (Fig. 1 in Ref. [31]), when the size of voids became large enough to form *o*-Ps. Then this lifetime further increased to 1.1 ns. Defect formation energies were determined for those aromatic hydrocarbons. They varied from 0.2 ± 0.02 eV for biphenyl to 2.4 ± 0.3 eV for quaterphenyl. Since one should expect longer *o*-Ps lifetimes for vacancies in these molecular crystals, the nature of those defects and the mechanism by which they influence the Ps yield are not clear.

In the case of the supercooled Sm-*E* phase of 4TCB, an *o*-Ps lifetime of about 1.6 ns started to be observed at 163 K, as can be seen in Fig. 2(a). Thus the free volumes had a radius definitely larger than the threshold value sufficient for Ps formation, i.e., 0.12 nm [32,33]. This may suggest a change of the material properties at that temperature. In contrast, the character of the obtained temperature I_3 dependence is distinct and indicates a thermally activated process.

B. Annealing of the ordered crystalline phase

For temperatures lower than 198 K the positron lifetime spectra for the ordered crystalline phase exhibited only a single lifetime component, similarly to the Sm-*E* phase. The value of the single lifetime component related to positron annihilation from a free state increases slightly with temperature from 0.381 ± 0.001 to 0.388 ± 0.001 ns for the temperature range from 93 to 193 K and it is a few picoseconds lower than that for the supercooled Sm-*E* phase. Above this temperature the spectra exhibit three components. The second component, i.e., τ_2, coming from positron annihilation in a free state is a continuation of the single lifetime at lower temperatures and further increases smoothly to 0.411 ± 0.001 ns at 278 K and then more steeply to 0.470 ± 0.003 between 283 and 293 K. For the ordered crystalline phase, the τ_3 component appears at higher temperature, i.e., 198 K (open diamonds in Fig. 2), than

for the Sm-E phase. If the first few scattered points presenting τ_3 in Fig. 2(a), for which I_3 is lower than 1%, are omitted τ_3 is in the range between 1.8 and 1.9 ns up to a temperature of 278 K. These positron lifetimes correspond to the radii of the spherical free volume R in the range between 0.266 and 0.275 nm. Therefore, the size of the free volumes seen by positrons is smaller than that obtained for the Sm-E phase.

The o-Ps lifetime obtained from the relation given by Eq. (2) with the packing coefficient for the crystal phase $k = 0.75$ (the volume of the lattice cell was calculated according to Ref. [11]) is equal to 0.71 ns. Such a lifetime is not observed for 4TCB. Then the free volumes in the perfect structure of ordered crystalline phase are too small for Ps formation. The tight molecular packing of the crystalline phase is confirmed by the fact that only one molecular motion, i.e., the methyl reorientation, is observed for this phase. Additionally, the molecules are head-to-tail ordered [10]. The observed lifetime in the range between 1.8 and 1.9 ns can originate from the annihilation of o-Ps localized in open volume (hole-type) defects of molecular size.

Considering the grain boundaries as defects confining Ps, one should take into account the positron and Ps diffusion lengths, which are ~0.1 μm and ~2 nm, respectively. This usually causes the empty space between the grains for powder materials or imperfections of the grain boundaries to be too macroscopic to be detected using Ps as a probe. It seems that the value of $2R$ corresponds well with size of the 4TCB molecule in the direction perpendicular to its long axis, which is given by the size of the benzene rings. Thus this lifetime component may originate from the annihilation of o-Ps localized in molecular vacancies. Since the molecules are elongated, vacancies should be described by cylindrical or cuboid shapes. For the cuboid case the appropriate formula combining the o-Ps pickoff annihilation lifetime τ_{po} (in ns) with the free volume dimensions is [33]

$$\tau_{po} = \frac{1}{2}\left(1 - \prod_{i=1}^{3}\{a_i/(a_i + 2\Delta R) + (1/\pi)\sin[\pi a_i/(a_i + 2\Delta R)]\}\right)^{-1}, \quad (5)$$

where a_1, a_2, and a_3 are the cuboid edge lengths. The dimensions of the cuboid void calculated for the o-Ps lifetime are comparable with the 4TCB molecule dimensions. The good agreement was obtained for $\Delta R = 0.19$ nm. This value of ΔR was proposed in Ref. [33] for molecular crystals with channel-like free volumes. For the o-Ps lifetime of 1.9 ns the dimensions of the cuboid are equal to $0.46 \times 0.46 \times 1.7$ nm^3. The increase of the o-Ps lifetime from 1.8 to 1.9 ns may be caused by the thermal expansion of the crystal lattice. The intensity of this component increased linearly to 4% at 278 K, as shown in Fig. 2(b), which may reflect an increase of vacancy concentration with temperature.

As can be seen in Fig. 2(a), above 278 K, τ_3 for the ordered crystalline sample increases and reaches a value of 2.21 ns, which is characteristic of the Sm-E phase at 288 K. The intensity I_3 depicted in Fig. 2(b) increases steeply from 4% to 21%, which also is the value characteristic of the Sm-E phase. Changes of τ_3 and I_3 indicate that the transition between the ordered crystalline and the Sm-E phase took place between 283 and 288 K, which is in agreement with the value of 284.1 K obtained from the heat capacity measurements [10]. This kind of change in τ_3 and I_3 was observed for phase transformations from the ordered crystalline to the liquid crystalline phase [5,14]. An increase of τ_3 can be well understood within the bubble model of Ps formation.

C. Fast measurements on cooling and heating of the sample during preparation for crystallization

The fast measurement for the sample in the Sm-E phase was described in Sec. II. Figure 5 presents the number of counts in the chosen time interval, which is related mainly to the intensity of the o-Ps component of the positron lifetime spectra, as a function of the temperature for cooling (down-pointing black triangles) and then heating from 93 to 253 K with the same rate (up-pointing gray triangles). It also shows the number of counts as a function of time for the isothermal process for the sample kept at 253 K (closed circles). The first two dependences exhibit hysteresis. It is not complete because heating of the sample was stopped at a temperature of 253 K before reaching its initial value. Also shown in Fig. 5 is the temperature dependence of the number of counts obtained from the spectra for the annealing of the Sm-E phase (open squares), which were measured for 1 h and analyzed conventionally and for which the τ_3 and I_3 dependences are shown in Fig. 2. It should be noted that this dependence is

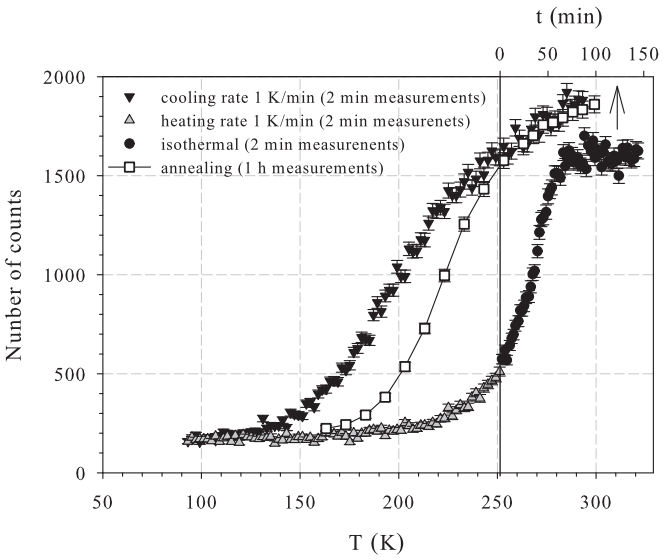

FIG. 5. Number of counts in the time range of the positron lifetime spectrum between 2.2 and 8.2 ns (shown in Fig. 1) as a function of the temperature for Sm-E cooling from 293 to 93 K and heating from 93 to 253 K with a rate of 1 K/min and the number of counts for the Sm-E phase kept at a temperature of 253 K as a function of time. Time is displayed on the upper horizontal axis in the right part separated by vertical black line. The spectra were registered for 2 min. Also shown is the temperature dependence of the number of counts obtained from the spectra for the annealing of the Sm-E phase, which were measured for 1 h and analyzed conventionally and for which the τ_3 and I_3 dependences are shown in Fig. 2.

the closest to equilibrium of three temperature dependences depicted in Fig. 5.

For the sample kept at 253 K, the number of counts increases during the first hour and then reaches the value obtained for cooling or for the 1-h measurement cycle and this value remains constant within the experimental error. This indicates that the sample reached the equilibrium.

D. Crystallization of the Sm-*E* phase of 4TCB

The dependences of τ_3 and I_3 on time for the isothermal measurement at 248 K after annealing of the sample at a temperature of 253 K for 48 h and lowering its temperature to 248 K are depicted in Fig. 6. The lifetime τ_3 decreases from 2.15 to 1.8 ns [Fig. 6(a)]. Its intensity decreases from 17.7% to 4% [Fig. 6(b)]. If the decrease of I_3 can be attributed to crystallization, the volume fraction of the ordered crystalline phase x may be related to the I_3 value. The volume fraction of the ordered crystalline phase x may be described by the Avrami equation for a phase transition at constant temperature:

$$x = 1 - \exp(-kt^n), \tag{6}$$

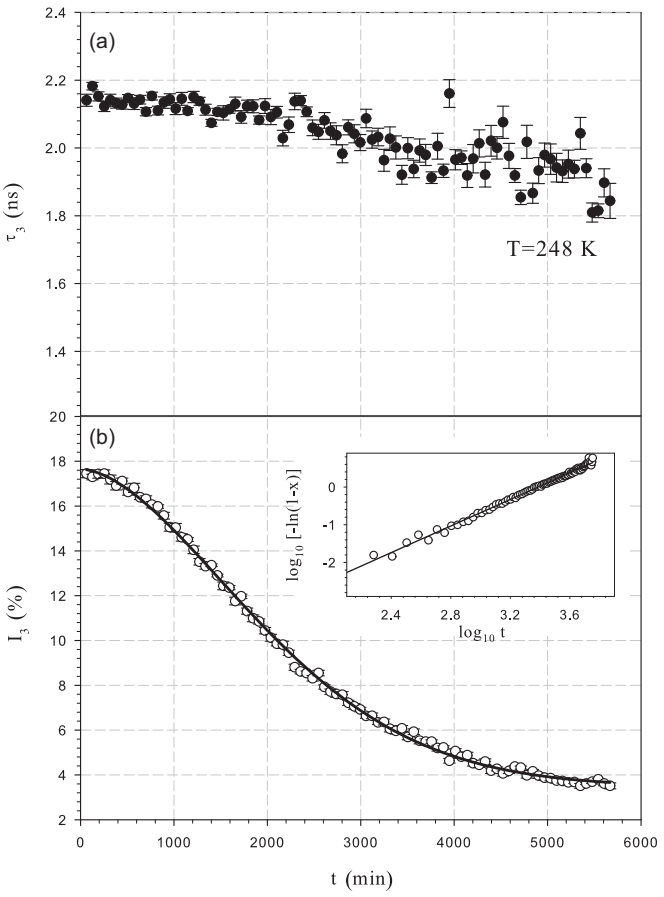

FIG. 6. Dependences of (a) τ_3 and (b) I_3 on time for the Sm-*E* phase of 4TCB for isothermal crystallization at a temperature of 248 K. The solid line represents the best fit of the relation given by Eq. (7) to the experimental points. The plot of $\log_{10}[-\ln(1-x)]$ as a function of $\log_{10} t$, where t is time, is shown in the inset.

where $0 \leqslant x \leqslant 1$, t is time, n is the Avrami exponent or order parameter reflecting the dimensionality of crystal growth, and k is a kinetic parameter depending on crystal nucleation and growth rate. Taking into account that at $t = 0$, $x = 0$ for $I_3 = 17.65\%$, i.e., the sample is entirely in the Sm-*E* phase, and x is related to I_3 linearly in the following way: $x = a(1 - I_3/100) + b$, where a and b are constants that are proportional and I_3 is expressed as a decimal fraction, which may be described by

$$I_3/100 = 1 - \frac{1 - \exp(-kt^n) - b}{a}. \tag{7}$$

The solid line in Fig. 6 was obtained by fitting this equation to the experimental points. For convenience, the inset in Fig. 6(b) shows the same experimental data in the form of a log-log plot with the fitted dependence $\log_{10}[-\ln(1-x)] = n\log_{10}(t) + \log_{10} k$. It can be seen that a single Avrami equation describes the experimental data very well. The parameters obtained from the fit are $n = 1.73 \pm 0.02$, $k = (2.8 \pm 0.6) \times 10^{-9}$ s^{-n}, and $\tau_{cr} = k^{-1/n} = (8.8 \pm 1.8) \times 10^4$ s.

The Avrami exponent n provides qualitative information on the nature of nucleation and growth processes. Low Avrami exponents correspond to growth of a low-dimensional crystal; e.g., disklike growth from instantaneous nuclei or rodlike growth from sporadic nuclei give an n value close to 2. Studies of crystallization kinetics performed for other liquid crystals exhibiting a Sm-*E* phase, i.e., *p*-phenyl-benzylidene-*p*′-heptylaniline and *p*-phenyl-benzylidene-*p*′-dodecylaniline, performed by Kumar *et al.* [34], gave even lower values of n that were ascribed to diffusion-controlled transformations with the initial growth of particles in the form of plates or needles. Values of the Avrami exponents close to that for 4TCB were obtained for *N*-(*p*-*n*-alkyoxybenzylidene)-*p*-*n*-alkylanilines (*n*O.*m* compounds), which crystallize from the smectic-*G* (Sm-*G*) phase [35]. In that case, the proposed mechanism of crystallization was described as sporadic nucleation and growth in two dimensions by forming ordered domains in smectic layers and propagation of this order to adjacent layers. Generally, smectic phases such as Sm-*G* with molecules tilted with respect to the director exhibit lower rates of crystallization in comparison to the Sm-*E* phases. However, this does not explain why crystallization of 4TCB from the Sm-*E* phase is not easily performed and its rate is low in comparison to the other compounds of the *n*TCB homologous series. Crystallization of 6TCB was observed using infrared spectroscopy [36] and dielectric relaxation [37]. On cooling a glassy state of the Sm-*E* phase of 6TCB is formed and then on heating above the softening of the glass a metastable Sm-*E* phase crystallizes. A reasonable fit of the crystallization curve from dielectric relaxation measurements was obtained for the sum of two Avrami processes with the Avrami exponents lower than unity [37]. This was explained as crystallization of two ordered crystalline phases since 6TCB shows two such stable phases. If 4TCB does not exhibit polymorphism in the solid state then one Avrami process describing crystallization is quite justified.

IV. CONCLUSION

The study demonstrates the sensitivity of positron annihilation parameters to structural changes related to phase transitions in molecular materials. In 4TCB, the lifetime of *o*-Ps and its intensity respond to the phase transformation from the ordered crystalline phase to the Sm-*E* liquid crystalline phase showing an abrupt increase.

For the ordered crystalline phase the *o*-Ps lifetime observed with an intensity lower than 5% was ascribed to *o*-Ps annihilation in molecular vacancies. The values of the *o*-Ps lifetime in the Sm-*E* liquid crystalline phase of 4TCB was explained by the formation of a bubble induced by Ps, which confirms the liquidlike state of the butyl chains of molecules. The temperature dependence of the *o*-Ps intensity for the supercooled Sm-*E* phase may be explained by thermal generation of sites where bubbles are formed. This may be related to activation of molecular motions. It seems that head-to-tail disorder may also play some role. However, a detailed explanation of this behavior requires further studies. It would be interesting to see the change in positron lifetime parameters caused by a change in the orientational order of the molecules induced, for example, by an external electric field. The positron lifetime measurements for the supercooled Sm-*E* phase do not allow one to draw a conclusion on the formation of the Sm-*E* phase glass state.

We have observed isothermal crystallization of a liquid crystalline phase using positron lifetime spectroscopy. The assumption that the *o*-Ps intensity decrease was caused by the decrease of the Sm-*E* phase volume fraction enabled us to describe the obtained dependence using a single Avrami equation with an Avrami exponent equal to 1.73, which suggests low-dimensional crystal growth.

[1] *Positron Spectroscopy of Solids, in Proceedings of the International School of Physics "Enrico Fermi," Course CXXV, Varenna, 1993*, edited by A. Dupasquier and A. T. Mills, Jr. (IOS, Amsterdam, 1995).

[2] O. E. Mogensen, *Positron Annihilation in Chemistry* (Springer, Berlin, 1995).

[3] *Positron and Positronium Chemistry*, edited by D. M. Schrader and Y. C. Jean, Studies in Physical and Theoretical Chemistry Vol. 57 (Elsevier Science, Amsterdam, 1988).

[4] K. Chandramani Singh, Phys. Status Solidi C **6**, 2482 (2009).

[5] J. B. Nicholas and H. J. Ache, J. Chem. Phys. **57**, 1597 (1971).

[6] G. Dlubek, D. Bamford, I. Wilkinson, K. Borisch, M. Ashraf Alam, and C. Tschierske, Liq. Cryst. **26**, 863 (1999).

[7] S. Urban, K. Czupryński, K. Dąbrowski, J. Janik, H. Kresse, and H. Schmalfuss, Liq. Cryst. **28**, 691 (2001).

[8] M. Jasiurkowska, A. Budziak, J. Czub, M. Massalska-Arodź, and S. Urban, Liq. Cryst. **35**, 513 (2008).

[9] M. Massalska-Arodź, A. Wurflinger, and D. Busing, Z. Naturforsch. A **54**, 675 (1999).

[10] S. Ishimaru, K. Saito, S. Ikeuchi, M. Massalska-Arodź, and W. Witko, J. Phys. Chem. B **109**, 10020 (2005).

[11] E. Juszyńska, W. Zając, and M. Massalska-Arodź (unpublished).

[12] M. Massalska-Arodź, H. Schmalfuss, W. Witko, H. Kresse, and A. Wülflinger, Mol. Liq. Cyst. Liq. Cyst. **28**, 221 (2001).

[13] M. Jasiurkowska, A. Budziak, J. Czub, and S. Urban, Acta Phys. Pol. A **110**, 759 (2006).

[14] G. Dlubek, V. Bondarenko, I. Y. Al-Qaradawi, D. Kilburn, and R. Krause-Rehberg, Macromol. Chem. Phys. **205**, 512 (2004).

[15] G. Dlubek, in *Polymer Physics: From Suspensions to Nanocomposites and Beyond*, edited by L. A. Utracki and A. M. Jamieson (Wiley, Hoboken, NJ, 2010), p. 421.

[16] J. Bartoš, M. Iskrová-Miklošovičová, D. Cangialosi, A. Alegría, O. Šauša, H. Švajdlenková, A. Arbe, J. Krištiak, and J. Colmenero, J. Phys.: Condens. Matter **24**, 155104 (2012).

[17] J. Kansy, Nucl. Instrum. Methods Phys. Res. Sect. A **374**, 235 (1996).

[18] N. Djourelov and M. Misheva, J. Phys.: Condens. Matter **8**, 2081 (1996).

[19] T. Hirade, T. Oka, N. Morishita, A. Idesaki, and A. Shimada, Mater. Sci. Forum **733**, 151 (2013).

[20] S. J. Tao, J. Chem. Phys. **56**, 5499 (1972).

[21] M. Eldrup, D. Lightbody, and J. N. Sherwood, Chem. Phys. **63**, 51 (1981).

[22] D. Lightbody, J. N. Sherwood, and M. Eldrup, Chem. Phys. **93**, 475 (1985).

[23] R. A. Ferrell, Phys. Rev. **108**, 167 (1957).

[24] H. Schüring, C. Thieme, and R. Stannarius, Liq. Cryst. **28**, 241 (2001).

[25] K. Horiuchi, Y. Yamamura, R. Pełka, M. Sumita, S. Yasuzuka, M. Massalska-Arodź, and K. Saito, J. Phys. Chem. B **114**, 4870 (2010).

[26] Y. Yamamura, T. Adachi, T. Miazawa, K. Horiuchi, M. Sumita, M. Massalska-Arodź, S. Urban, and K. Saito, J. Phys. Chem. B **116**, 9255 (2012).

[27] J. P. Perdew, K. Burke, and M. Ernzerhof, Phys. Rev. Lett. **77**, 3865 (1996).

[28] A. D. Becke, Phys. Rev. A **38**, 3098 (1988).

[29] C. Lee, W. Yang, and R. G. Parr, Phys. Rev. B **37**, 785 (1988).

[30] Ch. Zhao and Y. Ujhira, J. Radioanal. Nucl. Chem. **211**, 137 (1996).

[31] T. Goworek, C. Rybka, J. Wawryszczuk, and R. Wasiewicz, Chem. Phys. Lett. **106**, 482 (1984).

[32] J. Dryzek, Acta Phys. Pol. A **95**, 539 (1999).

[33] B. Jasińska, A. E. Kozioł, and T. Goworek, Acta Phys. Pol. A **95**, 557 (1999).

[34] P. A. Kumar, Pisupati Swathi, and V. G. K. M. Pisipati, Z. Naturforsch. Teil A **57**, 226 (2002).

[35] T. Chitravel, M. L. N. Madhu Mohan, and V. Krishnakumar, Physica B **404**, 1310 (2009).

[36] M. Jasiurkowska, P. M. Zieliński, M. Massalska-Arodź, Y. Yamamura, and K. Saito, J. Phys. Chem. B **115**, 12327 (2011).

[37] M. Jasiurkowska, Ph.D. thesis, Institute of Nuclear Physics PAN, 2009.